1 # Routine monitoring of Western Lake Erie to track water quality

2 # changes associated with cyanobacterial harmful algal blooms

3
4 Anna G. Boegehold[1], Ashley M. Burtner[1], Andrew C. Camilleri[1], Glenn Carter[1], Paul DenUyl[1],
5 David Fanslow[2], Deanna Fyffe Semenyuk[1,3], Casey M. Godwin[1], Duane Gossiaux[2], Thomas H.
6 Johengen[1], Holly Kelchner[1], Christine Kitchens[1], Lacey A. Mason[2], Kelly McCabe[1], Danna
7 Palladino[2], Dack Stuart[1,4], Henry Vanderploeg[2], Reagan Errera[2]
8
9
10 [1]Cooperative Institute for Great Lakes Research (CIGLR), University of Michigan, 4840 South
11 State Road, Ann Arbor, MI 48108, USA
12 [2]NOAA Great Lakes Environmental Research Laboratory, 4840 South State Road, Ann Arbor,
13 MI 48108, USA
14 [3]Jacobs, 1999 Bryan Street, Suite 1200, Dallas, TX, 75201, USA
15 [4]Woods Hole Group, Inc., 107 Waterhouse Road, Bourne, MA 02532
16
17 *Correspondence to:* Anna G Boegehold (annaboeg@umich.edu) & Reagan Errera
18 (reagan.errera@noaa.gov)

Abstract

The western basin of Lake Erie has a history of recurrent cyanobacterial harmful algal blooms (HABs) despite decades of efforts by the United States and Canada to limit nutrient loading, a major driver of the blooms. In response, the National Oceanic and Atmospheric Administration (NOAA) Great Lakes Environmental Research Laboratory (GLERL) and the Cooperative Institute for Great Lakes Research (CIGLR) created an annual sampling program to detect, monitor, assess, and predict HABs in western Lake Erie. Here we describe the data collected from this monitoring program from 2012 to 2021. This dataset includes observations on physico-chemical properties, major nutrient fractions, phytoplankton pigments, microcystins, and optical properties for western Lake Erie. This dataset is particularly relevant for creating models, verifying and calibrating remote sensing algorithms, and informing experimental research to further understand the water quality dynamics that enable HABs in this internationally significant body of freshwater. The dataset can be freely accessed from NOAA National Centers for Environmental Information (NCEI) at https://doi.org/10.25921/11da-3x54 (Cooperative Institute for Great Lakes Research, University of Michigan; NOAA Great Lakes Environmental Research Laboratory, 2019).

Earth System
Science
Data

Introduction

35

36   Lake Erie is situated on the international boundary between the United States and

37 Canada and is the smallest by volume of the five Laurentian Great Lakes. It is ecologically,

38 culturally, and economically significant to the approximately 12.5 million people who live in the

39 watershed. Each year Lake Erie supports nearly 14,000 tonnes of commercial and traditional

40 fisheries, over 33,000,000 tonnes of freight, and over $1.5 million in recreation and tourism

41 business (Sterner et al., 2020). Lake Erie has endured multiple anthropogenic stressors since

42 European settlement in the area, most notably the draining of coastal wetlands for development

43 of agricultural lands in the late 18th century (Allinger and Reavie, 2013). Currently, the

44 ecological state of Lake Erie is considered poor, partially due to excess nutrient input that

45 supports harmful algal blooms (HABs; ECCC and US EPA, 2022). These seasonal HABs are

46 typically dominated by toxin producing cyanobacteria, causing concern for public and

47 ecosystem health (Watson et al., 2016). Humans can be exposed to cyanotoxins through

48 ingestion of contaminated fish and drinking water and through inhalation and dermal exposure

49 during recreational events such as swimming and boating (Carmichael and Boyer, 2016; Buratti

50 et al., 2017). Cyanotoxins can also cause illness and death in aquatic and terrestrial animals

51 (Carmichael and Boyer, 2016). The economic cost of HABs impacts in Lake Erie is estimated to

52 be hundreds of millions of dollars each year (Smith et al., 2019).

53   To combat the deteriorated state of Lake Erie water quality, bi-national water resource

54 management policies alongside scientific research and water quality monitoring efforts have

55 been underway for decades. The Great Lakes Water Quality Agreement (GLWQA), first signed

56 in 1972, was a commitment between the US and Canada in response to degraded water quality

57 throughout the Great Lakes ecosystem (GLWQA, 2012). Phosphorus was found to be the key

58 nutrient that was promoting excess phytoplankton growth (Charlton et al., 1993), and thus the

59 GLWQA sought to limit total phosphorus input to the lakes in an attempt to reduce

60   phytoplankton growth and biomass (Steffen et al., 2014). The 1972 Clean Water Act (CWA) was

61   similarly enacted to regulate pollution discharge, including phosphorus, into navigable waters in

62   the United States. After the signing and implementation of the phosphorus load reduction

63   practices outlined in the GLWQA and CWA, the water quality of Lake Erie improved and the

64   lake experienced a period of restoration (Makarewicz and Bertram, 1991). This success was

65   attributed to upgrades to sewage treatment plants and industrial discharges which reduced

66   phosphorus loading from point sources by 50% within ten years of peak levels observed in 1968

67   (Charlton et al., 1993; Joosse and Baker, 2011; Steffen et al., 2014).

68   While the water quality of Lake Erie rebounded in the 1980s and early 1990s, by the mid

69   1990s and early 2000s annual HAB events were occurring in Lake Erie again, particularly in the

70   warm, shallow western basin (Allinger and Reavie, 2013; Kane et al., 2015; Watson et al.,

71   2016). Total phosphorus loading has been relatively stable in Lake Erie from the 1980s onward

72   (Dolan and Chapra, 2012; Watson et al., 2016), and although phosphorus loading controls had

73   been a successful mitigation measure at one point, several anthropogenic stressors within the

74   watershed were exacerbating the issue of poor water quality. An increase in agricultural sources

75   of biologically available soluble nutrients, legacy phosphorus in the Lake Erie watershed, altered

76   nutrient cycling by invasive dreissenid mussels, and climate change are thought to be primarily

77   responsible for the HABs resurgence (Vanderploeg et al., 2001; Conroy et al., 2005; Bridoux et

78   al., 2010; Michalak et al., 2013; Matisoff et al., 2016; Huisman et al., 2018; Van Meter et al.,

79   2021).

80   The post-recovery period HABs have predominantly been composed of the

81   cyanobacteria species *Microcystis aeruginosa* along with genera *Anabaena, Aphanizomenon,*

82   *Dolichospermum,* and *Planktothrix* (Steffen et al., 2014; Watson et al., 2016). These

83   cyanobacteria can produce an array of several types of phycotoxins, with the most common

84   being a suite of hepatotoxins known as microcystins (MCs). Microcystins primarily affect the

85   liver but can also cause adverse health effects on the kidneys, brain, and reproductive organs

86   (Carmichael and Boyer, 2016). Phycotoxins are commonly present during Lake Erie HABs, and

87   in August 2014 the city of Toledo, OH drinking water supply was contaminated with MCs,

88   leaving >400,000 without clean drinking water (Steffen et al., 2017).

89   To understand HAB events in US waterways, Congress authorized the Harmful Algal

90   Bloom and Hypoxia Research and Control Act in 1998 (HABHRCA; Public Law 115-423) which

91   mandated the National Oceanic and Atmospheric Administration (NOAA) to "advance the

92   scientific understanding and ability to detect, monitor, assess, and predict HAB and hypoxia

93   events''. Under HABHRCA, the NOAA Great Lakes Environmental Research Lab (GLERL),

94   NOAA National Centers for Coastal Ocean Science (NCCOS), and the Cooperative Institute for

95   Great Lakes Research (CIGLR; formerly CILER - Cooperative Institute for Limnology and

96   Ecosystems Research) developed an ecological forecast to predict HAB events in Lake Erie.

97   Starting in 2008, researchers at these institutes began using remote sensing to monitor

98   seasonal HABs, created a seasonal forecast system based on spring P loads, and developed

99   models to predict short-term bloom changes to alert stakeholders and the public (Rowe et al.,

100   2016). Products from these efforts, known as Lake Erie Harmful Algal Bloom Forecasts, are

101   freely available during the bloom season at https://coastalscience.noaa.gov/research/stressor-

102   impacts-mitigation/hab-forecasts/lake-erie/.

103   *In-situ* sampling of the bloom was necessary to calibrate and validate the remote

104   sensing images and models as well as measure microcystin concentration. Sampling events

105   were led by personnel at GLERL and CIGLR starting in 2008 and were designed to collect

106   discrete samples within the extent of the bloom area. At first, samples were taken

107   opportunistically within the bloom and sampling locations and analytical parameters were

108   inconsistent. In 2009, regular sampling stations were identified based on spatial patterns of the

109   bloom. From 2009 to 2011, in addition to opportunistic samples, nine main stations in the

110   western basin of Lake Erie were sampled intermittently from June through October (Bertani et

111   al., 2017; Rowland et al., 2020). While these sampling efforts initially began to complement

112   existing research products, the experimental nature of the 2008 to 2011 sampling cruises also

113   provided insight into creating a regular monitoring program that would support critical research

114   and product development related to western Lake Erie HABs.

115   In 2012, researchers at GLERL and CIGLR, with support from the Great Lakes

116   Restoration Initiative (GLRI), formalized a sampling regimen to monitor the spatial and temporal

117   variability of seasonal HAB events in western Lake Erie (WLE). The establishment of this

118   monitoring program corresponded with increased federal emphasis on evaluating trends and

119   drivers of WLE HABs and water quality. Four monitoring stations were identified and regular

120   surface samples were collected from May to September and analyzed for nutrient, pigment, and

121   particulate microcystin concentrations (Figs. 1 & 2). In following years, the monitoring program

122   evolved and expanded. New stations were added to better characterize the bloom and

123   complement other observing systems. Sampling parameters were adjusted and added based on

124   the needs of current research (Table 1). Results of these sampling cruises were compiled and

125   distributed informally upon request until 2019 when the data were organized and archived on

126   the NOAA National Centers for Environmental Information (NCEI) open-access data repository

127   (https://www.ncei.noaa.gov/).

128   Long term monitoring of WLE is fundamental to the continual assessment of water

129   quality changes in response to both stressors and water quality management efforts (Hartig et

130   al., 2009, 2021). The GLERL/CIGLR monitoring data has been used by numerous researchers

131   to develop and assess models (Rowe et al., 2016; Weiskerger et al., 2018; Fang et al., 2019;

132   Liu et al., 2020; Qian et al., 2021; Wang and Boegman, 2021; Hellweger et al., 2022; Maguire et

133   al., 2022), to calibrate remote sensing algorithms (Sayers et al., 2016, 2019; Avouris and Ortiz,

134   2019; Bosse et al., 2019; Vander Woude et al., 2019; Pirasteh et al., 2020; Xu et al., 2022), and

135   to elucidate ecological mechanisms and complement experimental data (Cory et al., 2016;

136   Reavie et al., 2016; Berry et al., 2017; Steffen et al., 2017; Kharbush et al., 2019, 2023; Newell

137   et al., 2019; Den Uyl et al., 2021; Smith et al., 2021, 2022; Hoffman et al., 2022; Marino et al.,

138   2022; Yancey et al., 2022a, b).

139   The objective of this paper is to inform users of the dataset "Physical, chemical, and

140   biological water quality monitoring data to support detection of Harmful Algal Blooms (HABs) in

141   western Lake Erie, collected by the Great Lakes Environmental Research Laboratory and the

142   Cooperative Institute for Great Lakes Research since 2012" by describing the data generated

143   from this monitoring program and detailing how samples were collected and analyzed. This

144   paper contextualizes this long-term data set so that it can continue to be used to benefit our

145   collective ecological knowledge of western Lake Erie.

146

147   Table 1. Description of stations sampled in western Lake Erie from 2012 to 2021. Latitude and

148   longitude (decimal degree) coordinates for each station are target locations as the boat was

149   allowed to drift at each site during *in-situ* sampling.

150

Station	Latitude	Longitude	Avg. Depth (m)	Years Monitored
WE02	41.762	-83.330	5.4	2012-2021
WE04	41.827	-83.193	8.4	2012-2021
WE06	41.705	-83.385	2.9	2012-2021
WE08	41.834	-83.364	4.8	2012-2021
WE09	41.718	-83.424	2.7	2016-2021
WE12	41.703	-83.254	6.6	2014-2021
WE13	41.741	-83.136	8.9	2014-2021
WE14	41.720	-83.010	9.3	2015
WE15	41.617	-83.009	4.5	2015-2017
WE16	41.660	-83.143	6.2	2018-2021

151

Earth System
Science
Data

Methods

Study Site

Based on the lake's bathymetry, Lake Erie can be divided into the eastern, central, and western basins which in turn influence physical and biological processes (Allinger and Reavie, 2013). The data presented in this paper were collected from the western basin, which encompasses the western part of the lake to Point Pelee, ON, Canada and Cedar Point, OH, USA (Fig. 1). The well-mixed western basin is the shallowest (maximum average depth of 11 m), warmest, and most productive of the three basins. Although it's typical for temperate WLE to have ice cover in the winter (Jan to Mar), summer (Jul to Sep) surface water temperatures often reach or exceed 25 °C. The western basin receives 95% of its hydraulic inflow from the Detroit River, which connects Lake Erie hydrologically to Lake Huron via the St. Clair River and Lake St. Clair (Cousino et al., 2015). Among the other tributaries to WLE (including River Raisin, Portage River, Ottawa River, Stony Creek, Swan Creek, and Sandusky River), the Maumee River discharges into the western basin near the city of Toledo, Ohio and contributes a significant amount of sediments and nutrients to the entire Lake Erie basin (Baker et al., 2014a, b). Nutrient and sediment loads from the Maumee River can vary with precipitation, where stormwater runoff can provide a pulse of nutrients into the basin, potentially altering cyanobacteria dynamics (Baker et al., 2014a; King et al., 2022). Land use in the Lake Erie watershed is 75% agricultural and 11% urban, both of which contribute to the large amounts of soluble reactive phosphorus into the basin (Mohamed et al., 2019; Myers et al., 2000).

This dataset includes water quality data from ten monitoring stations on the United States side of WLE that were sampled from 2012 to 2021 (Figs. 1 & 2, Tables 1 & 2). The average depth of monitoring stations ranged from 2.7 m at WE9 to 9.3 m at WE14. These sites

175   were chosen to reflect the various nutrient and hydrologic inputs and gradients into WLE, as

176   well as represent areas of the basin that are prone to HABs. The Maumee River inflow was a

177   major consideration in determining these sites. The initial 4 stations sampled in this program

178   (WE02, WE04, WE06, and WE08) were selected because they were consistently within the

179   WLE blooms occurring at the time. Additional sites were later added to better represent the

180   spatial extent of HABs and to augment existing data provided by moored buoy continuous

181   monitoring systems, advanced monitoring technologies, such as Environmental Sample

182   Processors (Den Uyl et al., 2022), and other monitoring programs in WLE.

Field Sampling

184   Western Lake Erie discrete field sampling was accomplished using NOAA GLERL

185   research vessels. Sampling took place during ice-free months and aimed to quantify the

186   environmental conditions prior to, during, and at the end of the bloom (Fig. 2). Sampling stations

187   represent approximate locations (Table 1; Fig. 1); *in situ* measurements and sampling were

188   collected once the boat reached the targeted location and then proceeded to drift during

189   sampling. The frequency and timing of those cruises varied over the first few years but has been

190   consistent since 2017 (Fig. 2). Sampling was disrupted in 2020 due to the global COVID-19

191   pandemic and resulting public health restrictions. In 2020, sampling was initiated in mid-June at

192   a reduced number of sites for select water quality parameters. In July, sampling stations and

193   parameters were expanded and all stations and parameters were sampled and measured by

194   August 2020. The prior standard sampling schedule resumed in April 2021.
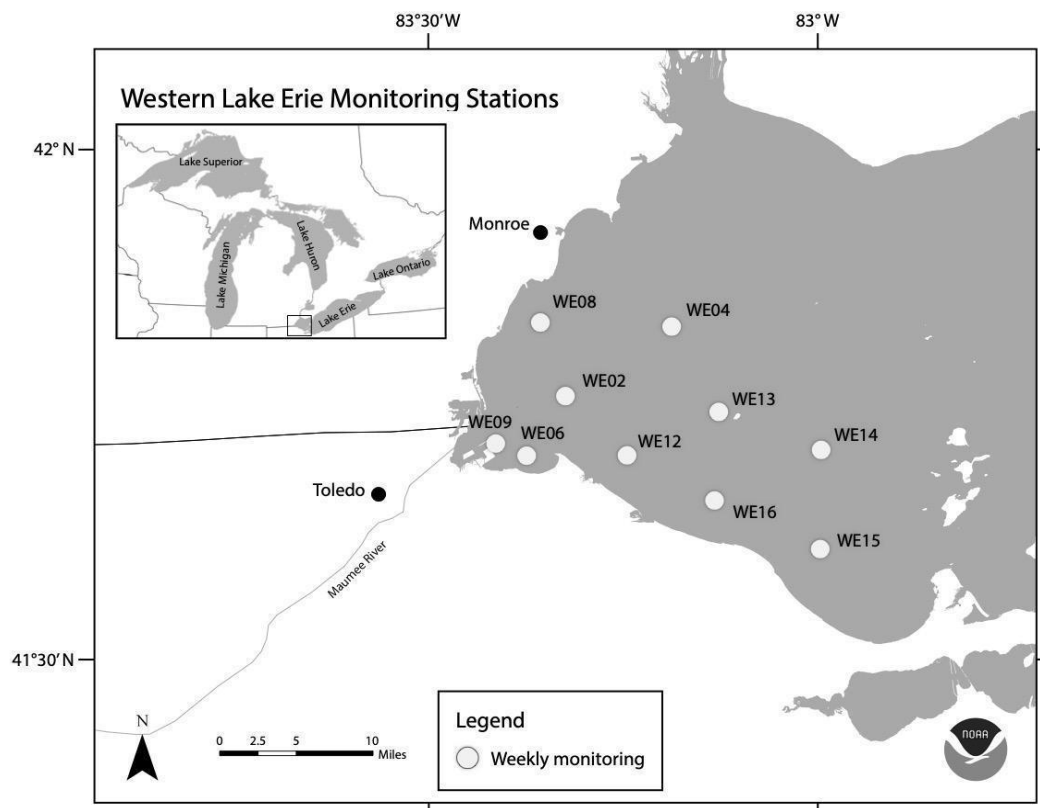
195

196   Figure 1. Location of western Lake Erie water quality monitoring stations. This map was

197   provided by NOAA for use in this publication.

Earth System
Open Access Science
Data Discussions

198
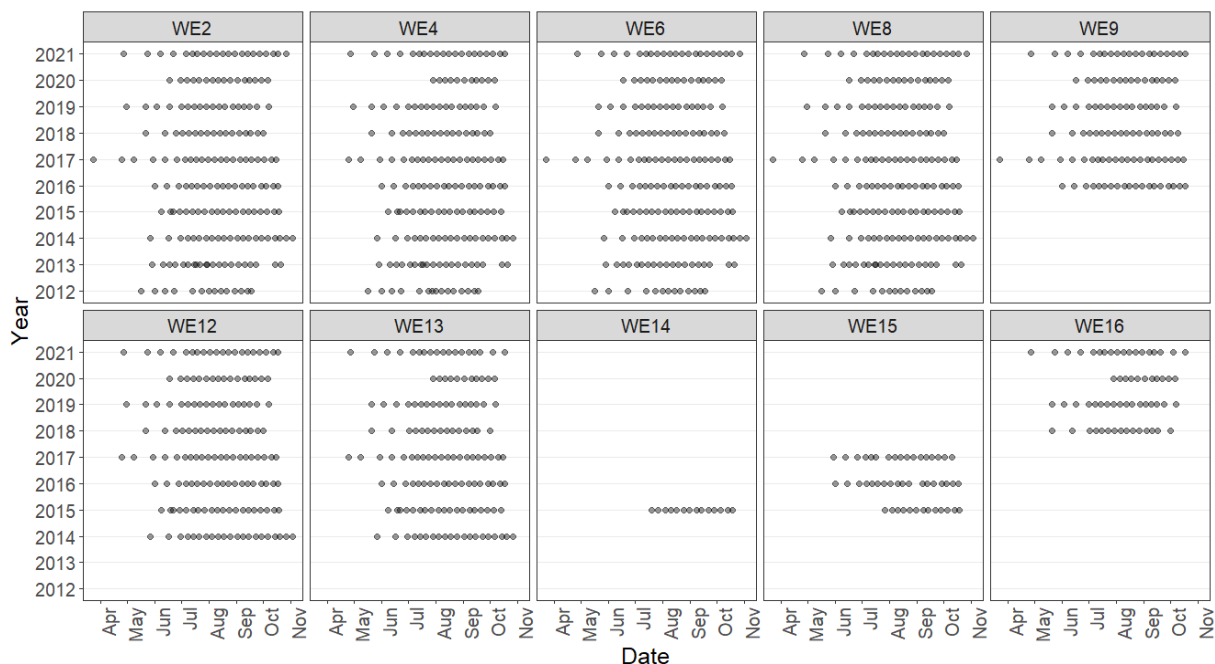
Figure 2. Sampling frequency for each monitoring station for years sampled between 2012 to
2021.

201

In-situ measurements for conductivity, temperature, dissolved oxygen (DO), beam

attenuation, transmission, and photosynthetically active radiation (PAR) were taken with a Sea-

Bird 19plus V2 conductivity, temperature, and depth (CTD) profiler attached to a hydraulic

crane. Data were collected on the downcast and were reported as the mean of recorded values

within ± 0.5 m of the discrete sample depth. In 2012, sample temperature was taken on the boat

with a Vee Gee Scientific IP67-rated digital thermometer. Sky conditions were recorded at the

discretion of the field technician at each station during the sampling cruise. A Secchi disk was

lowered into the water on the shaded side of the boat at each station and the depth at which the

Secchi disk was no longer visible was recorded (Wetzel and Likens, 2000).

Water column samples were collected using a 5 L vertical Niskin bottle (General

Oceanics model 1010). Niskin casts were evenly distributed between one or more high-density

213   polyethylene bottles that were rinsed with site water and stored in a cooler. Three to four Niskin

214   casts were used to fill the bottles, such that each bottle is a composite sample of the water

215   collected. Surface samples were taken 0.75 m below the water's surface, mid-column samples

216   were taken at approximately 4.25 m below surface, and benthic or bottom samples were taken

217   at approximately 0.5 m above the lake bottom at each station. Surface samples were taken at

218   all stations while mid-column and benthic sample collection varied between sites and years.

219   Scum samples of dense cyanobacterial accumulation on the surface of the water were collected

220   opportunistically using a 2 L modified Van Dorn water sampler. Sampling times were reported

221   as Eastern Daylight Time (UT -4:00). Upon arrival at the laboratory, raw water samples were

222   immediately subsampled and preserved until analysis.

223   Wind speed and wave height data were obtained from moored buoy continuous

224   monitoring systems in proximity to sampling stations for a timestamp that corresponded to the

225   time samples were collected at that station. Wave height data for all stations were obtained from

226   the Toledo Intake Buoy (owned and maintained by Limnotech Inc.). Wind speed data for

227   stations WE02, WE06, WE09, WE12, WE14, WE15, and WE16 were also collected from this

228   buoy. Data for this buoy is available through the Great Lakes Observing System (GLOS;

229   platform ID 45165, https://seagull.glos.org/data-console/71). Wind speed data for stations

230   WE04, WE08, and WE13 were obtained from the Toledo Harbor Light no. 2 buoy (Station

231   THLO1, owned and maintained by GLERL). Data for this buoy is available through NOAA's

232   National Data Buoy Center (https://www.ndbc.noaa.gov/station_realtime.php?station=THLO1).

233

234   Laboratory analysis of samples

235   Water collected from WLE was subsampled to make a range of analytical

236   measurements in the laboratory (Table 2).

237

238   Table 2. Summary of parameters reported in the dataset.

Parameter	Years monitored	Method
Surface samples	2012-2021	n/a
Mid-column samples	2015	n/a
Benthic samples	2015-2021	n/a
Station depth	2012-2021	Sea-Bird 19plus V2 CTD profiler
Time of sampling (Eastern Daylight Time UT -4:00)	2012-2021	n/a
Latitude (decimal degree)	2012-2021	n/a
Longitude (decimal degree)	2012-2021	n/a
Wind speed (knots)	2015-2021	Moored buoy continuous monitoring systems
Wave height (ft)	2012-2021	Moored buoy continuous monitoring systems
Cloud cover (sky)	2012-2021	n/a
Secchi depth (m)	2012-2021	Wetzel and Likens (2000)
Sample temperature (°C)	2012	Vee Gee Scientific digital thermometer
CTD temperature (°C)	2013-2021	Sea-Bird 19plus V2 CTD profiler
CTD specific conductivity (μS cm^{-1})	2013-2021	Sea-Bird 19plus V2 CTD profiler
CTD beam attenuation (m^{-1})	2013-2021	Sea-Bird 19plus V2 CTD profiler
CTD transmission (%)	2013-2021	Sea-Bird 19plus V2 CTD profiler
CTD dissolved oxygen (DO; mg L^{-1})	2013-2021	Sea-Bird 19plus V2 CTD profiler
CTD photosynthetically active radiation (PAR; μE m^{-2} s^{-1})	2013-2021	Sea-Bird 19plus V2 CTD profiler
Turbidity (NTU)	2013-2021	EPA Method 180.1
Particulate microcystins (μg L^{-1})	2012-2021	Wilson et al. (2008)
Dissolved microcystins (μg L^{-1})	2014-2021	Wilson et al. (2008)

Phycocyanin (µg L^{-1})	2012-2021	Horvath et al. (2013)
Chlorophyll a (µg L^{-1})	2012-2021	Speziale et al. (1984)
Total phosphorus (TP; µg L^{-1})	2012-2021	Standard Method 4500-P
Total dissolved phosphorus (TDP; µg L^{-1})	2012-2021	Standard Method 4500-P
Soluble reactive phosphorus (SRP; µg L^{-1})	2012-2021	Standard Method 4500-P
Ammonia (µg L^{-1})	2012-2021	Standard Method 4500-nh3-nitrogen (ammonia)
Nitrate + Nitrite (mg L^{-1})	2012-2021	Standard Method 4500-no3-nitrogen (nitrate)
Urea (µg L^{-1})	2016-2017	Milvenna and Savidge (1992), Goeyens et al. (1998), Chaffin and Bridgeman (2014)
Particulate organic carbon (POC; mg L^{-1})	2012-2021	Hedges and Stern (1984)
Particulate organic nitrogen (PON; mg L^{-1})	2012-2021	Hedges and Stern (1984)
Colored dissolved organic material (CDOM; m^{-1})	2014-2021	Binding et al. (2008), Mitchell et al. (2003)
Dissolved organic carbon (DOC; mg L^{-1})	2012-2017	APHA Standard Method 5310 B
Total suspended solids (TSS; mg L^{-1})	2012-2021	APHA Standard Method 2540
Volatile suspended solids (VSS; mg L^{-1})	2012-2021	APHA Standard Method 2540

239

Optical properties

241   Turbidity was measured on raw samples using a Hach 2100AN Turbidimeter following

242 US EPA method 180.1 (1993). Colored dissolved organic material (CDOM, also defined as

243 chromophoric dissolved organic matter) was determined by filtering lake water through an acid

244 rinsed 0.2 µm nuclepore polycarbonate filter into acid-washed and combusted borosilicate vials.

245 Optical density of the filtered samples was then measured using a Perkin Elmer UV/VIS

246   Lambda 35 spectrophotometer at wavelengths from 300-800 nm. CDOM absorption was

247   calculated at 400 nm (Mitchell et al., 2003; Binding et al., 2008).

248   Dissolved organic carbon (DOC) concentrations were determined following American

249   Public Health Association (APHA) Standard Method 5310 B. Briefly, lake water was filtered

250   through 0.45 µm polyvinylidene difluoride membrane filters into combusted borosilicate glass

251   vials and frozen at -20°C until analysis. The filtrate was acidified with HCl and sparged with air

252   for 6 min before being analyzed on a Shimadzu total organic carbon analyzer.

253   Duplicate samples for particulate organic carbon (POC) and particulate organic nitrogen

254   (PON) were collected onto pre-combusted glass fiber filters and analyzed following Hedges and

255   Stern (1984) Samples were stored at -20 °C until analysis. The filters were then acidified by

256   fumigation with 10% HCl and dried at 70°C for 24 h before being quantified on a Perkin Elmer

257   2400 or a Carlo-Erba 1110 CHN elemental analyzer.

258   Total suspended solids (TSS) and volatile suspended solids (VSS) were determined via

259   gravimetric analysis following APHA Standard Method 2540. A known volume of lake water was

260   filtered through a pre-combusted, pre-weighed Whatman GF/F glass fiber filter. The filters were

261   then dried at 60° C for at least 24 h and reweighed. The difference in mass between the pre-

262   weighed and processed filter was reported as TSS. Volatile suspended solids concentrations

263   were quantified by combusting the filters used for TSS analysis at 450 °C for 4 h, weighing the

264   combusted filters, and calculating the mass lost.

265   Nutrient fractions

266   Total phosphorus (TP) and total dissolved phosphorus (TDP) samples were collected in

267   duplicate by subsampling 50 mL (2012 to 2019) or 20 mL (2020 to 2021) of lake water into acid

268   washed glass tubes and by filtering 20 mL of lake water through a 0.2 µm membrane filter and

269   collecting the filtrate, respectively. Samples for TP and TDP were refrigerated until samples

270   were digested with potassium persulfate solution and autoclaved at 121°C for 30 min, modified

271   from APHA Standard Method 4500-P. Digested TP and TDP samples were stored at room

272   temperature until concentrations were measured on a Seal QuAAtro continuous segmented flow

273   analyzer (SEAL Analytical Inc.) from 2012 to 2019 and a Seal AA3 from 2020 to 2021 using the

274   ascorbic acid molybdenum method as detailed by the instrument manual and APHA Standard

275   Method 4500-P. Analytical detection limits for the analyses were taken from the instrument

276   manufacturer's documentation.

277   Soluble reactive phosphorus (SRP), ammonia, nitrate + nitrite, and urea were each

278   determined by filtering 12 mL of lake water through a 0.2 µm membrane filter into 15 mL

279   centrifuge tubes during field sampling. Sample filtrates were stored at -20 °C upon receipt at the

280   laboratory. Soluble reactive phosphorus, ammonia, and nitrate + nitrite concentrations were

281   determined simultaneously on a Seal AA3 continuous segmented flow analyzer. Soluble

282   reactive phosphorus concentrations, like TP and TDP concentrations, were measured using the

283   ascorbic acid molybdenum method as detailed by the instrument manual and APHA Standard

284   Method 4500-P. Ammonia concentrations were measured using Bertholet reactions according

285   to the instrument manual and APHA Standard Method 4500-nh3-nitrogen. Nitrate + nitrite

286   concentrations were measured using copper-cadmium reduction methods according to the

287   instrument manual and APHA Standard Method 4500-no3-nitrogen. Analytical detection limits

288   for these inorganic nutrient analyses were taken from the instrument manufacturer's

289   documentation. Urea samples were measured by adding diacetyl monoxime and

290   thiosemicarbazide to the filtrate and briefly vortexing to mix, followed by adding sulfuric acid and

291   ferric chloride to the solution and briefly vortexing to mix. Samples were then incubated in the

292   dark for 72 h at room temperature before absorbance at 520 nm was read on a Perkin Elmer

293   UV/VIS Lambda 35 spectrophotometer. Urea concentrations were then quantified using a

294   standard curve (Mulvenna and Savidge, 1992; Goeyens et al., 1998; Chaffin and Bridgeman,

295   2014). The detection limit was calculated using the standard deviation of repeated

296   measurements.

Pigments and microcystins

297

298 Particulate phycocyanin and chlorophyll *a* concentrations were determined by filtering a

299 known volume of lake water under low vacuum (<200 mm Hg) onto 47 mm Whatman GF/F

300 glass fiber filters (Cytiva Life Sciences). Particulate phycocyanin sample filters were stored in 15

301 mL conical polypropylene centrifuge tubes and chlorophyll *a* sample filters were stored in amber

302 glass vials at -20 °C until analysis. Analysis methods for particulate phycocyanin were derived

303 from Horváth et al. (2013) where 9 mL of phosphate buffer was added to sample tubes and samples

304 were agitated using a shaker at 5 °C for 15 min at 100 rpm then vortexed for 10 s each. To

305 encourage cell lysis, samples were subjected to three freeze/thaw cycles at -20 °C followed by

306 sonication for 20 min using a Fisher FS110 H sonicator. Fluorescence of the extracted samples was

307 measured using an Aquafluor 8000-010 fluorometer (Turner Designs) with excitation from 400-600

308 nm and emission filter of >595 nm. Particulate phycocyanin was calibrated annually against C-

309 Phycocyanin material from Sigma-Aldrich. Analysis methods for chlorophyll *a* were derived from

310 Speziale et al. (1984) where chlorophyll *a* was extracted from samples using dimethylformamide

311 and placed into a 65 °C water bath for 15 min. Samples were then cooled to room temperature

312 and vortexed for 15-20 s before being quantified using a 10 AU fluorometer (Turner Designs)

313 with excitation filter of 436 nm and emission at 680 nm. Phycocyanin and chlorophyll *a*

314 procedures were performed under low or green light to reduce pigment degradation within the cell.

315 Dissolved and particulate microcystins were quantified using a procedure adapted from

316 Wilson et al. (2008). Dissolved microcystins (dMC) were determined through duplicate samples

317 of ~ 2 mL filtrate that was passed through a 0.2 μm membrane filter and stored in glass vials at -

318 20 °C until analysis. Particulate microcystins (pMC) were collected by filtering a known volume

319 of lake water onto a Whatman GF/F glass fiber filter (2012 to 2015) or a 3 μm pore size

320 polycarbonate membrane filter (2016 to 2021). Particulate MC was then extracted from the

321 filters. In sampling years 2012 to 2015, glass fiber filters were submerged in a glass vial

322   containing a 75:25 methanol:water solution (MeOH/H$_2$O) and sonicated in an ice bath for 2 min.

323   The samples were centrifuged for 15 min and the supernatant was transferred to a clean glass

324   vial. An additional 5 mL of MeOH/H$_2$O was added to the filter/precipitate and the sample was

325   incubated at -20 °C for 5 h. The sample was then sonicated for 2 min, centrifuged, and the

326   supernatant was removed and added to the first extract vial. The composite supernatant was

327   then centrifuged under a vacuum until dry. The dried extract was then stored at -20 °C until

328   analysis. Particulate MC concentrations were then determined by adding 1 mL of MIlliQ water to

329   the sample and using sonication to dissolve the dried extract. For sampling years 2016 to 2021,

330   filters were stored in 2 mL sterile microcentrifuge tubes at -20 °C until analysis. During analysis,

331   pMC were extracted from the membrane filters by adding 1 mL of MilliQ water and subjecting

332   samples to three freeze/thaw cycles at -20 °C followed by addition of Abraxis QuickLyse

333   reagents according to the manufacturer (Eurofins/Abraxis). Particulate MC samples for all

334   sampling years were analyzed immediately after extraction. For all sampling years, dMC and

335   pMC concentrations were determined using a congener-independent enzyme-linked

336   immunosorbent assay (ELISA) kit designed to detect and quantity microcystins and nodularins

337   using the ADDA moiety (Envirologix brand used from 2012 to 2015; Eurofins/Abraxis

338   microcystins/nodularins (ADDA) (EPA ETV) (EPA method 546), ELISA, 96-test kit used from

339   2016 to 2021). Analytical detection limits for the analyses were taken from the manufacturer's

340   documentation.

Results and Discussion

341

342   This dataset demonstrates the temporal and spatial variability in water quality

343   parameters in western Lake Erie from 2012 to 2021. Overall, sites closer to the Maumee River

344   inflow (i.e., WE06 and WE09) had the highest median concentrations of nutrients, sediments,

345   pigments, and microcystins compared to sites further out in the basin (i.e., WE02, WE04, and

346   WE13; Table 3). Stations WE06 and WE04 were sampled since the initiation of the monitoring

347   program and consistently represented the high and low extremes of water quality observations

348   during a given time point, respectively, (Table 3) and select parameters for these two sites are

349   represented in figs. 3 and 4. Supplemental figs. 1-16 display the same parameters as figs. 3 and

350   4 for the remaining stations.

351

352
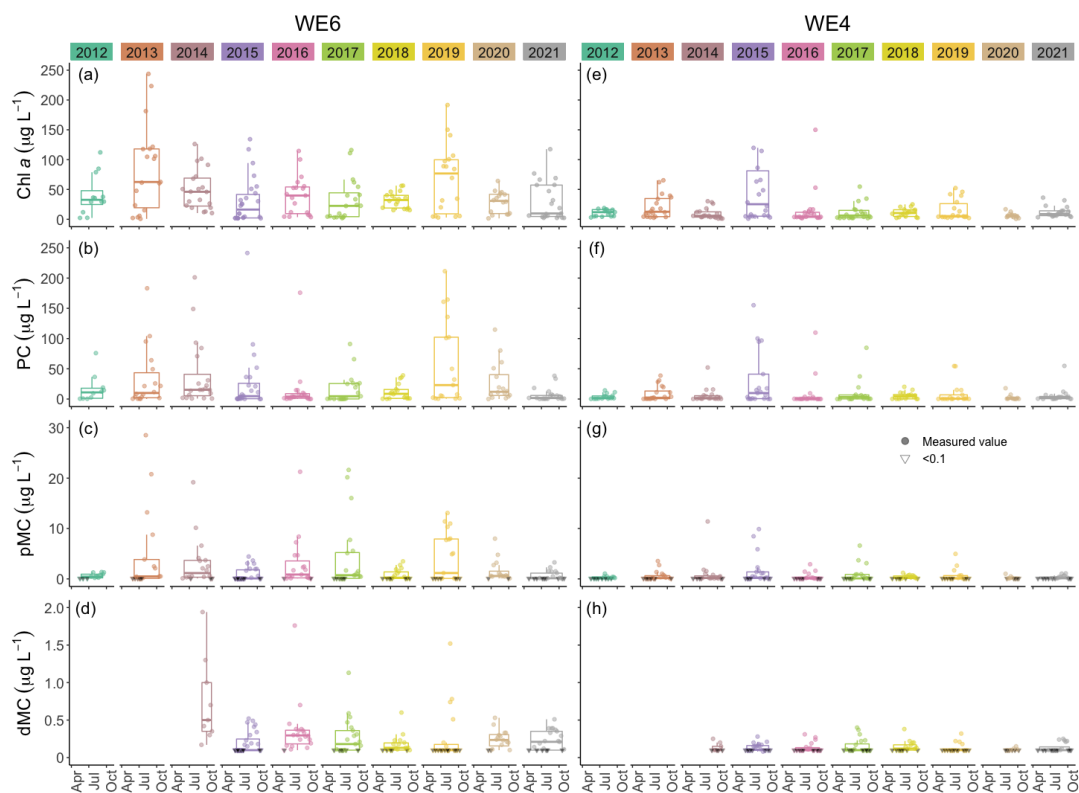
Fig 3. Comparison of chlorophyll *a* (Chl *a*), phycocyanin (PC), particulate microcystins (pMC),

and dissolved microcystins (dMC) between stations WE04 and WE06 from 2012 to 2021.

Boxplots represent the median and 25% and 75% quartiles with whiskers extending to the

highest or lowest point within 1.5x the interquartile range. A scatterplot is overlaid on the

boxplots.

Earth System
Science
Data
Open Access
Discussions
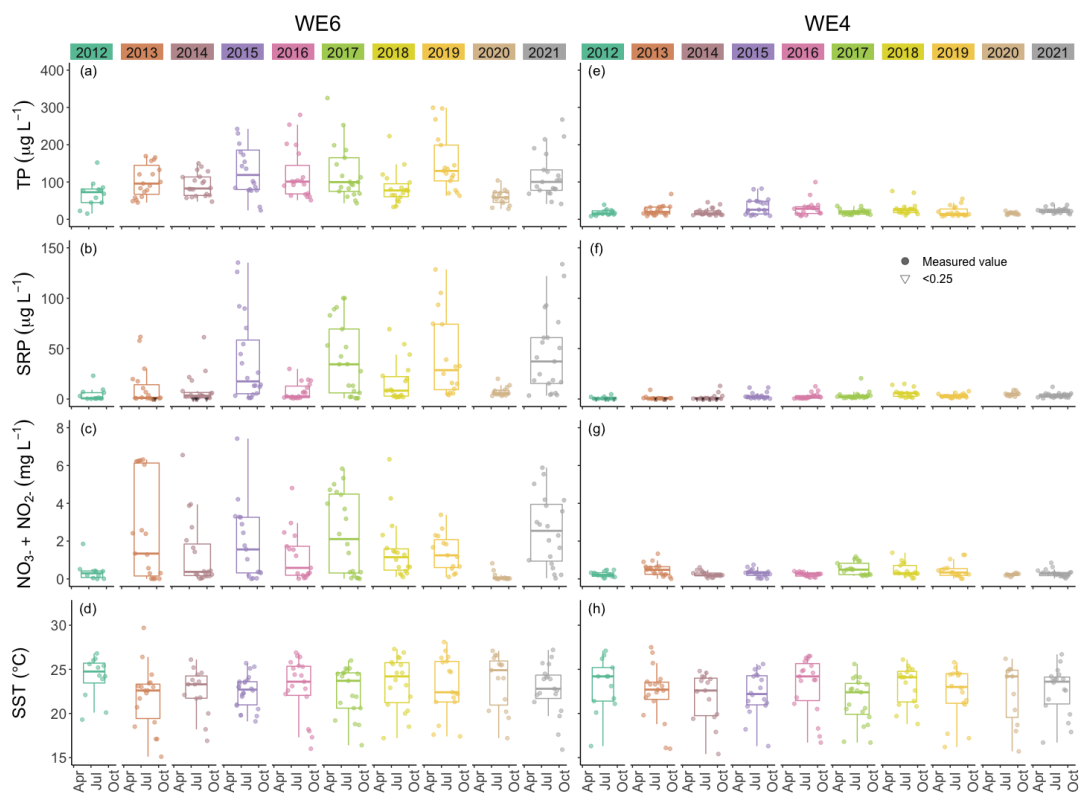
Fig 4. Comparison of total phosphorus (TP), soluble reactive phosphorus (SRP), nitrate plus nitrite (NO_3^- + NO_2^-), and sea surface temperature (SST) between stations WE04 and WE06 from 2012 to 2021. Boxplots represent the median and 25% and 75% quartiles with whiskers extending to the highest or lowest point within 1.5x the interquartile range. A scatterplot is overlaid on the boxplots.

Earth System Science Data Discussions
Open Access

366   Table 3. Median values of each parameter at each monitoring station for all surface samples

367   collected between 2012 to 2021.

	Secchi depth (m)	Temp. (°C)	Cond. (µS cm)	DO (mg L)	PAR (µE m⁻² s)	Beam Attenuation (m)	Transmission (%)	Turbidity (NTU)	Particulate MC (µg L)	Dissolved MC (µg L)	Phycocyanin (µg L)	Chl-a (µg L)	TP (µg L)	TDP (µg L)	SRP (µg L)	Ammonia (µg L)	Nitrate + Nitrite (mg L)	POC (mg L)	PON (mg L)	CDOM (m)
WE02	0.8	23.1	287	7.7	264	5.1	28.2	9.9	0.78	0.20	4.8	17.5	53.3	12.8	5.7	12.6	0.44	1.4	0.23	0.99
WE04	2.0	22.9	244	7.6	377	2.2	58.4	3.0	0.46	0.17	1.2	7.7	19.2	4.5	2.2	12.9	0.27	0.63	0.10	0.34
WE06	0.5	23.0	346	7.6	173	6.4	20.5	14.8	1.5	0.28	8.0	33.0	90.1	18.7	8.7	11.8	0.83	2.4	0.38	2.0
WE08	1.0	23.3	299	7.7	166	4.3	34.4	9.0	0.88	0.22	5.7	19.5	50.9	12.3	5.8	13.8	0.45	1.5	0.25	1.1
WE09	0.3	23.9	395	7.1	127	12.6	4.3	23.2	0.95	0.26	5.2	32.6	133	44.8	29.5	43.1	1.4	2.5	0.42	2.4
WE12	0.8	23.1	276	7.7	266	5.4	25.9	11.0	0.67	0.16	2.9	15.1	47.6	10.1	5.4	8.4	0.31	1.2	0.20	0.81
WE13	1.5	22.9	244	7.8	456	2.7	52.4	4.3	0.56	0.15	2.6	8.6	22.3	5.0	2.7	10.2	0.25	0.78	0.14	0.38
WE14	1.4	23.2	238	8.1	796	3.7	40.2	7.2	0.80	0.16	17.0	40.0	31.0	4.7	1.5	2.9	0.17	1.7	0.27	0.60
WE15	1.0	23.0	261	7.7	391	3.4	43.0	6.3	0.86	0.19	2.7	12.7	34.8	5.5	2.0	23.9	0.27	1.1	0.18	0.54
WE16	1.3	24.1	269	7.4	297	3.6	40.8	6.3	0.91	0.18	3.4	12.3	30.2	7.2	4.0	10.6	0.30	1.0	0.16	0.71

368

Physicochemical properties

370   Median surface temperatures for all samples across all years ranged from 22.9 to 24.1

371   °C and median benthic temperatures ranged from 22.8 to 23.2 °C (Table 3, Fig. 4), indicating

372   that WLE was thermally well mixed throughout the sampling period. A summary of the dataset

373   indicates that 23.8% of surface temperatures were ≥25 °C, and these higher temperatures all

374   occurred from mid-June through the end of September. Bloom forming cyanobacteria species in

375   Lake Erie, including *Microcystis spp.,* often reach maximum growth rates at warmer

376   temperatures (≥ 25 °C) than eukaryotic phytoplankton (Steffen et al., 2014; Huisman et al.,

377   2018). Despite having warmer temperatures that promote recurring HABs, there was only one

378   recorded instance of hypoxia (DO <2 mg L^{-1}) in the dataset and it occurred at WE13 on 08 July

379   2019. Median DO was 7.62 mg L^{-1} in all surface samples and 7.02 mg L^{-1} in all benthic samples

380   from 2012 to 2021 (Table 3), again indicating minimal stratification in WLE during sampling.

381   Median conductivity from 2012 to 2021 was highest at sites WE06 and WE09, which are closest

382   to the Maumee River input, and lowest at sites WE04 and WE13 near the middle of the basin

383   (Table 3). WE06 and WE09 were the only sites to have median conductivity values above 300

384   μS cm^{-1}.

Optical properties

386   Biotic and abiotic particulate concentrations and movement patterns in WLE are prone to

387   spatial and seasonal variations and are heavily influenced by loading from the Maumee River

388   (Prater et al., 2017; Maguire et al., 2022). Secchi depth, turbidity, and PAR measurements have

389   been correlated with distance from Maumee Bay, where light penetration was lowest near the

390   Maumee River (Chaffin et al., 2011). Variability in optical property measurements in WLE is also

391   dependent on Maumee River inputs, and changes in optical properties can potentially be used

392   in remote sensing algorithms to detect changes in water quality (Sayers et al., 2019). Median

393   Secchi disk depth over the entire dataset was highest at WE04 and lowest at WE06 and WE09,

394   which are closest to the Maumee River (Table 3). Other optical properties, such as PAR, beam

395   attenuation, and transmittance also followed this spatial pattern. In a summary of all samples,

396   median PAR measured at 0.5 m below surface was highest at WE13 and WE14 and lowest at

397   WE09; median transmittance was highest at WE04 and lowest at WE09; and median beam

398   attenuation and turbidity were highest at WE09 and lowest at WE04 (Table 3). Median turbidity

399   values at each site over the 2012 to 2021 period were within the range of previously reported

400   values in the WLE basin (Barbiero and Tuchman, 2004). Median CDOM absorbance and DOC,

401   TSS, and VSS concentrations were again highest at WE09 and lowest at WE04 (Table 3).

402   CDOM gradients in WLE are likewise affected by loading from the Maumee River (Cory et al.,

403   2016) and DOC and CDOM values from this dataset have been used as predictor variables in

404   models estimating PAR attenuation variation in WLE (Weiskerger et al., 2018).

Nutrient fractions

406   The Maumee River is a major contributor of nutrients to Lake Erie (Steffen et al., 2014;

407   Kast et al., 2021). Median TP concentrations in WLE from 2012 to 2021 were lowest at WE04

408   and highest at WE09 (Table 3, Fig. 4). Median concentrations at each station from 2012 to 2021

409   were above the GLWQA Annex 4 goals for TP concentration in open waters, which is 15 µg P L^{-1}

410   ^{1} for WLE. This goal was met in 92 of 1275 (7.2%) samples and these target values were

411   primarily recorded from stations WE04 and WE13. Sites closer to the mouth of the Maumee

412   River had higher median TP values. While TP loading from the Maumee River tributary declined

413   between 1982 to 2018 (Rowland et al., 2020) the proportion of dissolved P has increased

414   (Joosse and Baker, 2011; Stow et al., 2015). Median TDP values in the WLE dataset were

415   lowest at WE04 and highest at WE09 (Table 3) with a highest recorded value of 274 µg P L^{-1} at

416   WE08 in 2015. Median SRP concentrations for each station in this dataset were lowest at WE14

417   and WE15 and were highest at WE09 (Table 3). The maximum recorded SRP concentration

418   was 135.4 µg P L^{-1} at WE06 in 2015 (Fig. 4). Using this dataset, Newell et al. (2019) found that

419   the Maumee River N loading has become more chemically reduced over time where ammonium

420   and PON have increased. Median ammonia concentrations in WLE from 2012 to 2019 were

421   lowest at WE12 and WE14 and highest at WE09 (Table 3) with a recorded maximum

422   concentration of 2109 µg N L^{-1} at WE12 in 2017. Median nitrate + nitrite was lowest at WE13

423   and WE14 and highest at WE09 (Table 3), with a maximum recorded value of 9.5 mg N L^{-1} at

424   WE09 in 2016. See Fig. 4 for a comparison of nitrate + nitrite concentrations between WE04

425   and WE06. Median PON concentrations were lowest at WE04 and highest at WE09 (Table 3)

426   with a recorded max of 40.93 mg N L^{-1} at WE08 in 2015.

427 ## Pigments and microcystins

428   Median extracted chlorophyll *a* concentrations in surface waters from 2012 to 2021 were

429   lowest at WE04 and highest at WE06 (Table 3, Fig. 3). The highest recorded surface

430   concentration of chlorophyll *a* was 6784 µg L^{-1} on 10 August 2015 at WE08 during the most

431   severe bloom year in this dataset, according to the CI Index (Wynne et al., 2013; Lunetta et al.,

432   2015). The highest measured levels of particulate phycocyanin, pMC, and TP were also

433   recorded at WE06 on 10 August 2015. Other notably high chlorophyll *a* concentrations were

434   measured during severe bloom years in 2017 (532 µg L^{-1} at WE09 on 04 August) and 2019 (593

435   µg L^{-1} at WE09 on 05 August). Similarly, median surface particulate phycocyanin concentration

436   for 2012 to 2021 was highest at WE06 and lowest at WE04 (Table 3, Fig. 4). The highest

437   recorded phycocyanin value was from WE08 on 10 August 2015 (8228 µg L^{-1}), followed by 3315

438   µg L^{-1} at WE06 in 2013 during another severe bloom year.

439   Particulate MC concentrations had highest median concentrations at WE06 and were

440   lowest at WE04 (Table 3, Fig. 4), similar to particulate chlorophyll a and phycocyanin

441   observations. The highest recorded particulate MC concentration in this dataset was from 10

442   August 2015 at WE08 during a severe bloom year (297 µg L^{-1}), followed by 289 µg L^{-1} at WE06

443   in 2017 during another severe bloom year according to the CI Index (Wynne et al., 2013;

444   Lunetta et al., 2015). Median dMC concentrations were highest at WE06 and lowest at WE13

445   (Table 3). The maximum dissolved MC in the dataset was 8.19 µg L^{-1} at WE09 on 05 August

446   2019, which correlates with high chlorophyll a concentrations.

447   Although the United States does not federally enforce water quality criteria or regulations

448   for cyanotoxins in drinking water, the US EPA has a recommended health advisory of 1.6 µg L^{-1}

449   microcystins in drinking water for school-age children through adults (US EPA, 2015) while the

450   WHO and the Ohio EPA use 1 µg L^{-1} microcystins as a guideline (WHO, 2020). From 2012 to

451   2021, 44.4% of pMC samples in this dataset exceeded the WHO guidelines and 34.1%

452   exceeded the US EPA health advisory. Monitoring MC concentrations in western Lake Erie has

453   become especially pertinent since August 2014 when the Toledo, OH drinking water treatment

454   plant was contaminated with microcystins in excess of 1 µg L^{-1} and customers were alerted to

455   not drink their tap water until toxin levels were decreased (Steffen et al., 2017). The pMC

456   concentrations at our WLE monitoring stations varied from 1.2-10.1 µg L^{-1} on 04 August 2014

457   during this crisis.

458

Data Availability

459

460   The entire dataset detailed in this manuscript can be freely accessed through the NOAA

461   National Centers for Environmental Information (NCEI) data repository at

462   https://www.ncei.noaa.gov/. The data collection is titled "Physical, chemical, and biological water

463   quality monitoring data to support detection of Harmful Algal Blooms (HABs) in western Lake

464   Erie, collected by the Great Lakes Environmental Research Laboratory and the Cooperative

465   Institute for Great Lakes Research since 2012". The digital object identifier is

466   https://doi.org/10.25921/11da-3x54. The data presented in this manuscript are available in three

467   separate accession files within this collection including: 2012 to 2018 data is available under

468   NCEI Accession 0187718 v2.2 at https://www.ncei.noaa.gov/archive/accession/0187718; 2019

469   data is available under NCEI Accession 0209116 v1.1 at

470   https://www.ncei.noaa.gov/archive/accession/0209116; 2020 to 2021 data is available under

471   NCEI Accession 0254720 v1.1 at https://www.ncei.noaa.gov/archive/accession/0254720

472   (Cooperative Institute for Great Lakes Research, University of Michigan; NOAA Great Lakes

473   Environmental Research Laboratory, 2019). Future data will be added to this collection as it

474   becomes available.

Open Access Earth System Science Data Discussions

Conclusions

475

476   The western Lake Erie data collected and compiled by NOAA GLERL and CIGLR

477   represent ten years of routine water quality monitoring to detect, track, and predict

478   cyanobacterial HAB events in an area of the Great Lakes that has experienced significant

479   environmental degradation. While this monitoring initiative started in conjunction with remote

480   sensing efforts, it eventually became a standalone program. This ongoing program provides a

481   service to the region and contributes data for investigating the nuanced dynamics of potentially

482   toxic HABs fueled by excess nutrient loading into the WLE basin. For instance, this dataset has

483   assisted in assessing progress toward binational nutrient loading reduction efforts on lake basin

484   concentrations of phosphorus. Long-term monitoring programs like this one provide consistent

485   data which is useful for identifying patterns and variations within the ecosystem and in

486   determining the root cause of those changes. As the sites and parameters of this monitoring

487   program have already changed to adapt to the needs of research, this program will continue to

488   evolve as we consider adding parameters that encompass other aspects of bloom dynamics.

489   For example, lake samples can be analyzed for genomic data that will provide insights on the

490   ability of the current phytoplankton community to produce microcystins. This decadal history has

491   already been an invaluable resource for the research community, and it will continue to enrich

492   our collective scientific knowledge of water quality dynamics in western Lake Erie.

493

Acknowledgements

494

500

501

Author Contributions

503 Anna G Boegehold prepared the manuscript. Ashley M. Burtner performed field sampling,

504 laboratory processing, data processing, QA/QC and data management, manuscript revision,

505 data curation. Andrew Camilleri performed field sampling, laboratory processing, manuscript

506 revision. Glenn Carter performed field sampling, laboratory processing, data processing,

507 methodology. Paul DenUyl performed field sampling, laboratory processing, manuscript

508 revision. David Fanslow performed field sampling, laboratory processing. Deanna Fyffe

509 Semenyuk performed field sampling, laboratory processing, manuscript revision. Casey Godwin

510 was responsible for project administration, supervision, visualization, manuscript revision,

511 methodology, field sampling, sample processing. Duane Gossiaux performed field sampling,

512 laboratory processing, manuscript revision, methodology. Tom Johengen was responsible for

513 project administration, supervision, field sampling, methodology. Holly Kelchner performed field

514 sampling, laboratory processing, manuscript revision. Christine Kitchens performed field

515 sampling, laboratory processing, data processing, manuscript revision. Lacey A. Mason was

516 responsible for data curation, manuscript revision. Kelly McCabe performed field sampling,

517 laboratory processing, manuscript revision, methodology. Danna Palladino performed field

518 sampling, laboratory processing, data processing, manuscript revision. Dack Stuart performed

519 field sampling, data processing. Henry Vanderploeg was responsible for project administration,

520 supervision. Reagan Errera was responsible for project administration, supervision,

521 Visualization, manuscript revision, methodology.

522

Competing Interests

The authors declare that they have no conflict of interest

References

Allinger, L. E. and Reavie, E. D.: The ecological history of Lake Erie as recorded by the phytoplankton community, J. Gt. Lakes Res., 39, 365–382, https://doi.org/10.1016/j.jglr.2013.06.014, 2013.

Avouris, D. M. and Ortiz, J. D.: Validation of 2015 Lake Erie MODIS image spectral decomposition using visible derivative spectroscopy and field campaign data, J. Gt. Lakes Res., 45, 466–479, https://doi.org/10.1016/j.jglr.2019.02.005, 2019.

Baker, D. B., Ewing, D. E., Johnson, L. T., Kramer, J. W., Merryfield, B. J., Confesor, R. B., Peter Richards, R., and Roerdink, A. A.: Lagrangian analysis of the transport and processing of agricultural runoff in the lower Maumee River and Maumee Bay, J. Gt. Lakes Res., 40, 479–495, https://doi.org/10.1016/j.jglr.2014.06.001, 2014a.

Baker, D. B., Confesor, R., Ewing, D. E., Johnson, L. T., Kramer, J. W., and Merryfield, B. J.: Phosphorus loading to Lake Erie from the Maumee, Sandusky and Cuyahoga rivers: The importance of bioavailability, J. Gt. Lakes Res., 40, 502–517, https://doi.org/10.1016/j.jglr.2014.05.001, 2014b.

Barbiero, R. P. and Tuchman, M. L.: Long-term Dreissenid Impacts on Water Clarity in Lake Erie, J. Gt. Lakes Res., 30, 557–565, https://doi.org/10.1016/S0380-1330(04)70371-8, 2004.

Berry, M. A., Davis, T. W., Cory, R. M., Duhaime, M. B., Johengen, T. H., Kling, G. W., Marino, J. A., Den Uyl, P. A., Gossiaux, D., Dick, G. J., and Denef, V. J.: Cyanobacterial harmful algal blooms are a biological disturbance to Western Lake Erie bacterial communities, Environ. Microbiol., 19, 1149–1162, https://doi.org/10.1111/1462-2920.13640, 2017.

Bertani, I., Steger, C. E., Obenour, D. R., Fahnenstiel, G. L., Bridgeman, T. B., Johengen, T. H., Sayers, M. J., Shuchman, R. A., and Scavia, D.: Tracking cyanobacteria blooms: Do different monitoring approaches tell the same story?, Sci. Total Environ., 575, 294–308, https://doi.org/10.1016/j.scitotenv.2016.10.023, 2017.

Binding, C. E., Jerome, J. H., Bukata, R. P., and Booty, W. G.: Spectral absorption properties of dissolved and particulate matter in Lake Erie, Remote Sens. Environ., 112, 1702–1711, https://doi.org/10.1016/j.rse.2007.08.017, 2008.

Bosse, K. R., Sayers, M. J., Shuchman, R. A., Fahnenstiel, G. L., Ruberg, S. A., Fanslow, D. L., Stuart, D. G., Johengen, T. H., and Burtner, A. M.: Spatial-temporal variability of in situ cyanobacteria vertical structure in Western Lake Erie: Implications for remote sensing observations, J. Gt. Lakes Res., 45, 480–489, https://doi.org/10.1016/j.jglr.2019.02.003, 2019.

Bridoux, M., Sobiechowska, M., Perez-Fuentetaja, A., and Alben, K. T.: Algal pigments in Lake Erie dreissenids, pseudofeces and sediments, as tracers of diet, selective feeding and bioaccumulation, J. Gt. Lakes Res., 36, 437–447, https://doi.org/10.1016/j.jglr.2010.06.005, 2010.

Buratti, F. M., Manganelli, M., Vichi, S., Stefanelli, M., Scardala, S., Testai, E., and Funari, E.: Cyanotoxins: producing organisms, occurrence, toxicity, mechanism of action and human health

563   toxicological risk evaluation, Arch. Toxicol., 91, 1049–1130, https://doi.org/10.1007/s00204-016-
564   1913-6, 2017.

565   Carmichael, W. W. and Boyer, G. L.: Health impacts from cyanobacteria harmful algae blooms:
566   Implications for the North American Great Lakes, Harmful Algae, 54, 194–212,
567   https://doi.org/10.1016/j.hal.2016.02.002, 2016.

568   Chaffin, J. D. and Bridgeman, T. B.: Organic and inorganic nitrogen utilization by nitrogen-
569   stressed cyanobacteria during bloom conditions, J. Appl. Phycol., 26, 299–309,
570   https://doi.org/10.1007/s10811-013-0118-0, 2014.

571   Chaffin, J. D., Bridgeman, T. B., Heckathorn, S. A., and Mishra, S.: Assessment of Microcystis
572   growth rate potential and nutrient status across a trophic gradient in western Lake Erie, J. Gt.
573   Lakes Res., 37, 92–100, https://doi.org/10.1016/j.jglr.2010.11.016, 2011.

574   Charlton, M. N., Milne, J. E., Booth, W. G., and Chiocchio, F.: Lake Erie Offshore in 1990:
575   Restoration and Resilience in the Central Basin, J. Gt. Lakes Res., 19, 291–309,
576   https://doi.org/10.1016/S0380-1330(93)71218-6, 1993.

577   Conroy, J. D., Kane, D. D., Dolan, D. M., Edwards, W. J., Charlton, M. N., and Culver, D. A.:
578   Temporal Trends in Lake Erie Plankton Biomass: Roles of External Phosphorus Loading and
579   Dreissenid Mussels, J. Gt. Lakes Res., 31, 89–110, https://doi.org/10.1016/S0380-
580   1330(05)70307-5, 2005.

581   Cooperative Institute for Great Lakes Research, University of Michigan; NOAA Great Lakes
582   Environmental Research Laboratory: Physical, chemical, and biological water quality monitoring
583   data to support detection of Harmful Algal Blooms (HABs) in western Lake Erie, collected by the
584   Great Lakes Environmental Research Laboratory and the Cooperative Institute for Great Lakes
585   Research since 2012, NOAA National Centers for Environmental Information [data set],
586   https://doi.org/10.25921/11da-3x54, 2019.

587   Cory, R. M., Davis, T. W., Dick, G. J., Johengen, T., Denef, V. J., Berry, M. A., Page, S. E.,
588   Watson, S. B., Yuhas, K., and Kling, G. W.: Seasonal Dynamics in Dissolved Organic Matter,
589   Hydrogen Peroxide, and Cyanobacterial Blooms in Lake Erie, Front. Mar. Sci., 3, 2016.

590   Cousino, L. K., Becker, R. H., and Zmijewski, K. A.: Modeling the effects of climate change on
591   water, sediment, and nutrient yields from the Maumee River watershed, J. Hydrol. Reg. Stud., 4,
592   762–775, https://doi.org/10.1016/j.ejrh.2015.06.017, 2015.

593   Den Uyl, P. A., Harrison, S. B., Godwin, C. M., Rowe, M. D., Strickler, J. R., and Vanderploeg,
594   H. A.: Comparative analysis of Microcystis buoyancy in western Lake Erie and Saginaw Bay of
595   Lake Huron, Harmful Algae, 108, 102102, https://doi.org/10.1016/j.hal.2021.102102, 2021.

596   Den Uyl, P. A., Thompson, L. R., Errera, R. M., Birch, J. M., Preston, C. M., Ussler, W. I.,
597   Yancey, C. E., Chaganti, S. R., Ruberg, S. A., Doucette, G. J., Dick, G. J., Scholin, C. A., and
598   Goodwin, K. D.: Lake Erie field trials to advance autonomous monitoring of cyanobacterial
599   harmful algal blooms, Front. Mar. Sci., 9, https://doi.org/10.3389/fmars.2022.1021952, 2022.

600   Dolan, D. M. and Chapra, S. C.: Great Lakes total phosphorus revisited: 1. Loading analysis
601   and update (1994–2008), J. Gt. Lakes Res., 38, 730–740,
602   https://doi.org/10.1016/j.jglr.2012.10.001, 2012.

603 Environment and Climate Change Canada and the U.S. Environmental Protection Agency.
604 2022. State of the Great Lakes 2022 Technical Report. Cat No. En161-3/1E-PDF. EPA 905-
605 R22-004. Available at binational.net, 2022.

606 Fang, S., Del Giudice, D., Scavia, D., Binding, C. E., Bridgeman, T. B., Chaffin, J. D., Evans, M.
607 A., Guinness, J., Johengen, T. H., and Obenour, D. R.: A space-time geostatistical model for
608 probabilistic estimation of harmful algal bloom biomass and areal extent, Sci. Total Environ.,
609 695, 133776, https://doi.org/10.1016/j.scitotenv.2019.133776, 2019.

610 Goeyens, L., Kindermans, N., Abu Yusuf, M., and Elskens, M.: A Room Temperature Procedure
611 for the Manual Determination of Urea in Seawater, Estuar. Coast. Shelf Sci., 47, 415–418,
612 https://doi.org/10.1006/ecss.1998.0357, 1998.

613 Hartig, J. H., Zarull, M. A., Ciborowski, J. J. H., Gannon, J. E., Wilke, E., Norwood, G., and
614 Vincent, A. N.: Long-term ecosystem monitoring and assessment of the Detroit River and
615 Western Lake Erie, Environ. Monit. Assess., 158, 87–104, https://doi.org/10.1007/s10661-008-
616 0567-0, 2009.

617 GLWQA: Great Lakes Water Quality Agreement; Protocol Amending the Agreement Between
618 Canada and the United States of America on Great Lakes Water Quality, 1978, as Amended on
619 October 16, 1983 and on November 18, 1987, https://binational. net/2012/09/05/2012-glwqa-
620 aqegl/ (last access: November 2022), 2012.
621
622 Hartig, J. H., Francoeur, S. N., Ciborowski, J. J. H., Gannon, J. E., Sanders, C. E., Galvao-
623 Ferreira, P., Knauss, C. R., Gell, G., and Berk, K.: An ecosystem health assessment of the
624 Detroit River and western Lake Erie, J. Gt. Lakes Res., 47, 1241–1256,
625 https://doi.org/10.1016/j.jglr.2021.05.008, 2021.

626 Hedges, J. I. and Stern, J. H.: Carbon and nitrogen determinations of carbonate-containing
627 solids1, Limnol. Oceanogr., 29, 657–663, https://doi.org/10.4319/lo.1984.29.3.0657, 1984.

628 Hellweger, F. L., Martin, R. M., Eigemann, F., Smith, D. J., Dick, G. J., and Wilhelm, S. W.:
629 Models predict planned phosphorus load reduction will make Lake Erie more toxic, Science,
630 376, 1001–1005, https://doi.org/10.1126/science.abm6791, 2022.

631 Hoffman, D. K., McCarthy, M. J., Boedecker, A. R., Myers, J. A., and Newell, S. E.: The role of
632 internal nitrogen loading in supporting non-N-fixing harmful cyanobacterial blooms in the water
633 column of a large eutrophic lake, Limnol. Oceanogr., n/a, https://doi.org/10.1002/lno.12185,
634 2022.

635 Horváth, H., Kovács, A. W., Riddick, C., and Présing, M.: Extraction methods for phycocyanin
636 determination in freshwater filamentous cyanobacteria and their application in a shallow lake,
637 Eur. J. Phycol., 48, 278–286, https://doi.org/10.1080/09670262.2013.821525, 2013.

638 Huisman, J., Codd, G. A., Paerl, H. W., Ibelings, B. W., Verspagen, J. M. H., and Visser, P. M.:
639 Cyanobacterial blooms | Nature Reviews Microbiology, Nat. Rev. Microbiol., 16, 471–483,
640 https://doi.org/10.1038/s41579-018-0040-1, 2018.

641 Joosse, P. J. and Baker, D. B.: Context for re-evaluating agricultural source phosphorus
642 loadings to the Great Lakes, Can. J. Soil Sci., 91, 317–327, https://doi.org/10.4141/cjss10005,
643 2011.

644 Kane, D. D., Ludsin, S. A., Briland, R. D., Culver, D. A., and Munawar, M.: Ten+years gone:
645 Continued degradation of offshore planktonic communities in U.S. waters of Lake Erie's western
646 and central basins (2003–2013), J. Gt. Lakes Res., 41, 930–933,
647 https://doi.org/10.1016/j.jglr.2015.06.002, 2015.

648 Kast, J. B., Apostel, A. M., Kalcic, M. M., Muenich, R. L., Dagnew, A., Long, C. M., Evenson, G.,
649 and Martin, J. F.: Source contribution to phosphorus loads from the Maumee River watershed to
650 Lake Erie, J. Environ. Manage., 279, 111803, https://doi.org/10.1016/j.jenvman.2020.111803,
651 2021.

652 Kharbush, J. J., Smith, D. J., Powers, M., Vanderploeg, H. A., Fanslow, D., Robinson, R. S.,
653 Dick, G. J., and Pearson, A.: Chlorophyll nitrogen isotope values track shifts between
654 cyanobacteria and eukaryotic algae in a natural phytoplankton community in Lake Erie, Org.
655 Geochem., 128, 71–77, https://doi.org/10.1016/j.orggeochem.2018.12.006, 2019.

656 Kharbush, J. J., Robinson, R. S., and Carter, S. J.: Patterns in sources and forms of nitrogen in
657 a large eutrophic lake during a cyanobacterial harmful algal bloom, Limnol. Oceanogr., n/a,
658 https://doi.org/10.1002/lno.12311, 2023.

659 King, W. M., Curless, S. E., and Hood, J. M.: River phosphorus cycling during high flow may
660 constrain Lake Erie cyanobacteria blooms, Water Res., 222, 118845,
661 https://doi.org/10.1016/j.watres.2022.118845, 2022.

662 Liu, Q., Rowe, M. D., Anderson, E. J., Stow, C. A., Stumpf, R. P., and Johengen, T. H.:
663 Probabilistic forecast of microcystin toxin using satellite remote sensing, in situ observations and
664 numerical modeling, Environ. Model. Softw., 128, 104705,
665 https://doi.org/10.1016/j.envsoft.2020.104705, 2020.

666 Lunetta, R. S., Schaeffer, B. A., Stumpf, R. P., Keith, D., Jacobs, S. A., and Murphy, M. S.:
667 Evaluation of cyanobacteria cell count detection derived from MERIS imagery across the
668 eastern USA, Remote Sens. Environ., 157, 24–34, https://doi.org/10.1016/j.rse.2014.06.008,
669 2015.

670 Maguire, T. J., Stow, C. A., and Godwin, C. M.: Spatially referenced Bayesian state-space
671 model of total phosphorus in western Lake Erie, Hydrol. Earth Syst. Sci., 26, 1993–2017,
672 https://doi.org/10.5194/hess-26-1993-2022, 2022.

673 Makarewicz, J. C. and Bertram, P.: Evidence for the Restoration of the Lake Erie Ecosystem:
674 Water quality, oxygen levels, and pelagic function appear to be improving, BioScience, 41, 216–
675 223, https://doi.org/10.2307/1311411, 1991.

676 Marino, J. A., Denef, V. J., Dick, G. J., Duhaime, M. B., and James, T. Y.: Fungal community
677 dynamics associated with harmful cyanobacterial blooms in two Great Lakes, J. Gt. Lakes Res.,
678 48, 1021–1031, https://doi.org/10.1016/j.jglr.2022.05.007, 2022.

679 Matisoff, G., Kaltenberg, E. M., Steely, R. L., Hummel, S. K., Seo, J., Gibbons, K. J.,
680 Bridgeman, T. B., Seo, Y., Behbahani, M., James, W. F., Johnson, L. T., Doan, P., Dittrich, M.,
681 Evans, M. A., and Chaffin, J. D.: Internal loading of phosphorus in western Lake Erie, J. Gt.
682 Lakes Res., 42, 775–788, https://doi.org/10.1016/j.jglr.2016.04.004, 2016.

683   Michalak, A. M., Anderson, E. J., Beletsky, D., Boland, S., Bosch, N. S., Bridgeman, T. B.,
684   Chaffin, J. D., Cho, K., Confesor, R., Daloğlu, I., DePinto, J. V., Evans, M. A., Fahnenstiel, G. L.,
685   He, L., Ho, J. C., Jenkins, L., Johengen, T. H., Kuo, K. C., LaPorte, E., Liu, X., McWilliams, M.
686   R., Moore, M. R., Posselt, D. J., Richards, R. P., Scavia, D., Steiner, A. L., Verhamme, E.,
687   Wright, D. M., and Zagorski, M. A.: Record-setting algal bloom in Lake Erie caused by
688   agricultural and meteorological trends consistent with expected future conditions, Proc. Natl.
689   Acad. Sci., 110, 6448–6452, https://doi.org/10.1073/pnas.1216006110, 2013.

690   Mitchell, B.G., Kahru, M., Wieland, J., and Stramska, M.: Determination of spectral absorption
691   coefficients of particles, dissolved material and phytoplankton for discrete water samples, In:
692   Mueller, J.L., G.S. Fargion, and C.R. McClain [Eds.] Ocean Optics Protocols for Satellite Ocean
693   Color Sensor Validation, Revision 4, Volume IV: Inherent Optical Properties: Instruments,
694   Characterizations, Field Measurements and Data Analysis Protocols. NASA/TM- 2003-211621,
695   NASA Goddard Space Flight Center, Greenbelt, MD, Chapter 4, pp 39-64, 2003.

696   Mohamed, M. N., Wellen, C., Parsons, C. T., Taylor, W. D., Arhonditsis, G., Chomicki, K. M.,
697   Boyd, D., Weidman, P., Mundle, S. O. C., Cappellen, P. V., Sharpley, A. N., and Haffner, D. G.:
698   Understanding and managing the re-eutrophication of Lake Erie: Knowledge gaps and research
699   priorities, Freshw. Sci., 38, 675–691, https://doi.org/10.1086/705915, 2019.

700   Mulvenna, P. F. and Savidge, G.: A modified manual method for the determination of urea in
701   seawater using diacetylmonoxime reagent, Estuar. Coast. Shelf Sci., 34, 429–438,
702   https://doi.org/10.1016/S0272-7714(05)80115-5, 1992.

703   Myers, D.N., Thomas, M.A., Frey, J.W., Rheaume, S.J., and Button, D.T.: Water Quality in the
704   Lake Erie-Lake Saint Clair Drainages Michigan, Ohio, Indiana, New York, and Pennsylvania,
705   1996–98: U.S. Geological Survey Circular 1203, 35 p., https://pubs.water.usgs.gov/circ1203/,
706   2000.
707

708   Newell, S. E., Davis, T. W., Johengen, T. H., Gossiaux, D., Burtner, A., Palladino, D., and
709   McCarthy, M. J.: Reduced forms of nitrogen are a driver of non-nitrogen-fixing harmful
710   cyanobacterial blooms and toxicity in Lake Erie, Harmful Algae, 81, 86–93,
711   https://doi.org/10.1016/j.hal.2018.11.003, 2019.

712   Pirasteh, S., Mollaee, S., Fatholahi, S. N., and Li, J.: Estimation of Phytoplankton Chlorophyll-a
713   Concentrations in the Western Basin of Lake Erie Using Sentinel-2 and Sentinel-3 Data, Can. J.
714   Remote Sens., 46, 585–602, https://doi.org/10.1080/07038992.2020.1823825, 2020.

715   Prater, C., Frost, P. C., Howell, E. T., Watson, S. B., Zastepa, A., King, S. S. E., Vogt, R. J., and
716   Xenopoulos, M. A.: Variation in particulate C : N : P stoichiometry across the Lake Erie
717   watershed from tributaries to its outflow, Limnol. Oceanogr., 62, S194–S206,
718   https://doi.org/10.1002/lno.10628, 2017.

719   Qian, S. S., Stow, C. A., Rowland, F. E., Liu, Q., Rowe, M. D., Anderson, E. J., Stumpf, R. P.,
720   and Johengen, T. H.: Chlorophyll a as an indicator of microcystin: Short-term forecasting and
721   risk assessment in Lake Erie, Ecol. Indic., 130, 108055,
722   https://doi.org/10.1016/j.ecolind.2021.108055, 2021.

723   Reavie, E. D., Cai, M., Twiss, M. R., Carrick, H. J., Davis, T. W., Johengen, T. H., Gossiaux, D.,
724   Smith, D. E., Palladino, D., Burtner, A., and Sgro, G. V.: Winter–spring diatom production in

725 Lake Erie is an important driver of summer hypoxia, J. Gt. Lakes Res., 42, 608–618,
726 https://doi.org/10.1016/j.jglr.2016.02.013, 2016.

727 Rowe, M. D., Anderson, E. J., Wynne, T. T., Stumpf, R. P., Fanslow, D. L., Kijanka, K.,
728 Vanderploeg, H. A., Strickler, J. R., and Davis, T. W.: Vertical distribution of buoyant Microcystis
729 blooms in a Lagrangian particle tracking model for short-term forecasts in Lake Erie, J.
730 Geophys. Res. Oceans, 121, 5296–5314, https://doi.org/10.1002/2016JC011720, 2016.

731 Rowland, F. E., Stow, C. A., Johengen, T. H., Burtner, A. M., Palladino, D., Gossiaux, D. C.,
732 Davis, T. W., Johnson, L. T., and Ruberg, S.: Recent Patterns in Lake Erie Phosphorus and
733 Chlorophyll *a* Concentrations in Response to Changing Loads, Environ. Sci. Technol., 54, 835–
734 841, https://doi.org/10.1021/acs.est.9b05326, 2020.

735 Sayers, M., Fahnenstiel, G. L., Shuchman, R. A., and Whitley, M.: Cyanobacteria blooms in
736 three eutrophic basins of the Great Lakes: a comparative analysis using satellite remote
737 sensing, Int. J. Remote Sens., 37, 4148–4171, https://doi.org/10.1080/01431161.2016.1207265,
738 2016.

739 Sayers, M. J., Bosse, K. R., Shuchman, R. A., Ruberg, S. A., Fahnenstiel, G. L., Leshkevich, G.
740 A., Stuart, D. G., Johengen, T. H., Burtner, A. M., and Palladino, D.: Spatial and temporal
741 variability of inherent and apparent optical properties in western Lake Erie: Implications for
742 water quality remote sensing, J. Gt. Lakes Res., 45, 490–507,
743 https://doi.org/10.1016/j.jglr.2019.03.011, 2019.

744 Smith, D. J., Tan, J. Y., Powers, M. A., Lin, X. N., Davis, T. W., and Dick, G. J.: Individual
745 Microcystis colonies harbour distinct bacterial communities that differ by Microcystis oligotype
746 and with time, Environ. Microbiol., 23, 3020–3036, https://doi.org/10.1111/1462-2920.15514,
747 2021.

748 Smith, D. J., Berry, M. A., Cory, R. M., Johengen, T. H., Kling, G. W., Davis, T. W., and Dick, G.
749 J.: Heterotrophic Bacteria Dominate Catalase Expression during Microcystis Blooms, Appl.
750 Environ. Microbiol., 88, e02544-21, https://doi.org/10.1128/aem.02544-21, 2022.

751 Smith, R. B., Bass, B., Sawyer, D., Depew, D., and Watson, S. B.: Estimating the economic
752 costs of algal blooms in the Canadian Lake Erie Basin, Harmful Algae, 87, 101624,
753 https://doi.org/10.1016/j.hal.2019.101624, 2019.

754 Speziale, B. J., Schreiner, S. P., Giammatteo, P. A., and Schindler, J. E.: Comparison of N,N-
755 Dimethylformamide, Dimethyl Sulfoxide, and Acetone for Extraction of Phytoplankton
756 Chlorophyll, Can. J. Fish. Aquat. Sci., 41, 1519–1522, https://doi.org/10.1139/f84-187, 1984.

757 Standard Methods Committee of the American Public Health Association, American Water
758 Works Association, and Water Environment Federation: Standard Methods For the Examination
759 of Water and Wastewater, 23rd edition, Sections 2540 Solids, 4500-P Phosphorus, 4500-nh3-
760 nitrogen (ammonia), 4500-no3-nitrogen (nitrate), 5310 Total Organic Carbon, edited by: Lipps
761 WC, Baxter TE, Braun-Howland E, APHA Press, Washington, DC, ISBN 1625762402, 2017.

762 Steffen, M. M., Belisle, B. S., Watson, S. B., Boyer, G. L., and Wilhelm, S. W.: Status, causes
763 and controls of cyanobacterial blooms in Lake Erie, J. Gt. Lakes Res., 40, 215–225,
764 https://doi.org/10.1016/j.jglr.2013.12.012, 2014.

765   Steffen, M. M., Davis, T. W., McKay, R. M. L., Bullerjahn, G. S., Krausfeldt, L. E., Stough, J. M.
766   A., Neitzey, M. L., Gilbert, N. E., Boyer, G. L., Johengen, T. H., Gossiaux, D. C., Burtner, A. M.,
767   Palladino, D., Rowe, M. D., Dick, G. J., Meyer, K. A., Levy, S., Boone, B. E., Stumpf, R. P.,
768   Wynne, T. T., Zimba, P. V., Gutierrez, D., and Wilhelm, S. W.: Ecophysiological Examination of
769   the Lake Erie Microcystis Bloom in 2014: Linkages between Biology and the Water Supply
770   Shutdown of Toledo, OH, Environ. Sci. Technol., 51, 6745–6755,
771   https://doi.org/10.1021/acs.est.7b00856, 2017.

772   Sterner, R. W., Keeler, B., Polasky, S., Poudel, R., Rhude, K., and Rogers, M.: Ecosystem
773   services of Earth's largest freshwater lakes, Ecosyst. Serv., 41, 101046,
774   https://doi.org/10.1016/j.ecoser.2019.101046, 2020.

775   Stow, C. A., Cha, Y., Johnson, L. T., Confesor, R., and Richards, R. P.: Long-Term and
776   Seasonal Trend Decomposition of Maumee River Nutrient Inputs to Western Lake Erie, Environ.
777   Sci. Technol., 49, 3392–3400, https://doi.org/10.1021/es5062648, 2015.

778   US EPA - United States Environmental Protection Agency: Method 180.1: Determination of
779   Turbidity by Nephelometry, Revision 2.0, Edited by: O'Dell, J.W., 1993.

780   US EPA - United States Environmental Protection Agency: Drinking Water Health Advisory for
781   the Cyanobacterial Microcystin Toxins, EPA Document Number 820R15100, 2015.
782
783   Van Meter, K. J., McLeod, M. M., Liu, J., Tenkouano, G. T., Hall, R. I., Van Cappellen, P., and
784   Basu, N. B.: Beyond the Mass Balance: Watershed Phosphorus Legacies and the Evolution of
785   the Current Water Quality Policy Challenge, Water Resour. Res., 57, e2020WR029316,
786   https://doi.org/10.1029/2020WR029316, 2021.

787   Vander Woude, A., Ruberg, S., Johengen, T., Miller, R., and Stuart, D.: Spatial and temporal
788   scales of variability of cyanobacteria harmful algal blooms from NOAA GLERL airborne
789   hyperspectral imagery, J. Gt. Lakes Res., 45, 536–546,
790   https://doi.org/10.1016/j.jglr.2019.02.006, 2019.

791   Vanderploeg, H. A., Liebig, J. R., Carmichael, W. W., Agy, M. A., Johengen, T. H., Fahnenstiel,
792   G. L., and Nalepa, T. F.: Zebra mussel (Dreissena polymorpha) selective filtration promoted
793   toxic Microcystis blooms in Saginaw Bay (Lake Huron) and Lake Erie, Can. J. Fish. Aquat. Sci.,
794   58, 1208–1221, https://doi.org/10.1139/f01-066, 2001.

795   Wang, Q. and Boegman, L.: Multi-Year Simulation of Western Lake Erie Hydrodynamics and
796   Biogeochemistry to Evaluate Nutrient Management Scenarios, Sustainability, 13, 7516,
797   https://doi.org/10.3390/su13147516, 2021.

798   Watson, S. B., Miller, C., Arhonditsis, G., Boyer, G. L., Carmichael, W., Charlton, M. N.,
799   Confesor, R., Depew, D. C., Höök, T. O., Ludsin, S. A., Matisoff, G., McElmurry, S. P., Murray,
800   M. W., Peter Richards, R., Rao, Y. R., Steffen, M. M., and Wilhelm, S. W.: The re-eutrophication
801   of Lake Erie: Harmful algal blooms and hypoxia, Harmful Algae, 56, 44–66,
802   https://doi.org/10.1016/j.hal.2016.04.010, 2016.

803   Weiskerger, C. J., Rowe, M. D., Stow, C. A., Stuart, D., and Johengen, T.: Application of the
804   Beer–Lambert Model to Attenuation of Photosynthetically Active Radiation in a Shallow,
805   Eutrophic Lake, Water Resour. Res., 54, 8952–8962, https://doi.org/10.1029/2018WR023024,
806   2018.

807   Wetzel, R.G., and Likens G.E.: Limnological Analyses, 3rd edition, Springer New York, NY,
808   https://doi.org/10.1007/978-1-4757-3250-4, 2000.

809   WHO - World Health Organization: Cyanobacterial toxins: microcystins. Background document
810   for development of WHO Guidelines for drinking-water quality and Guidelines for safe
811   recreational water environments, WHO/HEP/ECH/WSH/2020.6, 2020.
812

813   Wilson, A. E., Gossiaux, D. C., Höök, T. O., Berry, J. P., Landrum, P. F., Dyble, J., and
814   Guildford, S. J.: Evaluation of the human health threat associated with the hepatotoxin
815   microcystin in the muscle and liver tissues of yellow perch (Perca flavescens), Can. J. Fish.
816   Aquat. Sci., 65, 1487–1497, https://doi.org/10.1139/F08-067, 2008.

817   Wynne, T. T., Stumpf, R. P., Tomlinson, M. C., Fahnenstiel, G. L., Dyble, J., Schwab, D. J., and
818   Joshi, S. J.: Evolution of a cyanobacterial bloom forecast system in western Lake Erie:
819   Development and initial evaluation, J. Gt. Lakes Res., 39, 90–99,
820   https://doi.org/10.1016/j.jglr.2012.10.003, 2013.

821   Xu, J., Liu, H., Lin, J., Lyu, H., Dong, X., Li, Y., Guo, H., and Wang, H.: Long-term monitoring
822   particulate composition change in the Great Lakes using MODIS data, Water Res., 222,
823   118932, https://doi.org/10.1016/j.watres.2022.118932, 2022.

824   Yancey, C.E., Mathiesen, O., and Dick, G.J.: Transcriptionally active nitrogen fixation and
825   biosynthesis of diverse secondary metabolites by Dolichospermum and Aphanizominom-like
826   Cyanobacteria in western Lake Erie Microcystis blooms, bioRxiv [preprint],
827   https://doi.org/10.1101/2022.09.30.510322 01 October 2022a.

828   Yancey, C. E., Smith, D. J., Den Uyl, P. A., Mohamed, O. G., Yu, F., Ruberg, S. A., Chaffin, J.
829   D., Goodwin, K. D., Tripathi, A., Sherman, D. H., and Dick, G. J.: Metagenomic and
830   Metatranscriptomic Insights into Population Diversity of Microcystis Blooms: Spatial and
831   Temporal Dynamics of mcy Genotypes, Including a Partial Operon That Can Be Abundant and
832   Expressed, Appl. Environ. Microbiol., 88, e02464-21, https://doi.org/10.1128/aem.02464-21,
833   2022b.